EUROTeV-Report-2005-020-1

Modelling of simple cases in view of active stabilisation for a future linear collider

B. Bolzon[2], L. Brunetti[1], N. Geffroy[2], C. Adloff[2], Y. Bastian[2], F. Cadoux[2], F. Formosa[3], C. Girard[2], A. Jeremie[2], Y. Karyotakis[2], J. Lottin[2]

October 24, 2005
Submitted to Nanobeam 2005

Abstract

Final focus magnet stabilisation is an important issue when working with nanometre size beams. The present study focuses on mechanical stabilisation. As a first step, the case of a 1m free-fixed aluminium beam placed on a table with active stabilisation has been studied. This work describes three aspects, namely, sensors and actuators to measure and compensate ground motion, mechanical simulations and a feedback loop. Measurements done with low frequency velocity sensors (down to 0.1Hz) in our Annecy lab during office hours show that the displacement RMS on the active table is 1nm at 4Hz compared to 10nm without active stabilisation.
Simulations of the dynamic response of the beam have been compared to measurements done with accelerometers placed on the clamping and on the free end of the aluminium beam. The results are in good agreement. We are therefore able to predict by simulation the response of a structure subjected to an external excitation. A first sketch of a feedback loop to compensate specific vibrations has also been developed and allows the simultaneous elimination of several resonance peaks on a reduced-size mock-up. This algorithm will be applied to stabilise a larger mock-up, leading to more realistic experimental conditions. In future tests, the active table will globally stabilise in a range of frequencies from 0.5Hz to 50Hz whereas the feedback loop will compensate single strong resonances.

[1] Laboratoire d'Informatique, Systèmes, Traitement de l'Information et de la Connaissance (LISTIC-ESIA), Université de Savoie, BP806 F-74016 Annecy Cedex, France
[2] Laboratoire d'Annecy-le-Vieux de Physique des Particules, LAPP-IN2P3-CNRS, BP110 F-74941Annecy-le-Vieux Cedex, France
[3] Laboratoire de Mécanique Appliquée (LMECA-ESIA), Université de Savoie, BP806 F-74016 Annecy Cedex, France

1 Introduction

Final focus magnet stabilisation is an important issue when working with nanometre size beams. Depending on the frequency range needed, this stabilisation can be achieved either by active mechanical stabilisation or by active beam based feedback. We are considering the requirements for mechanical stabilisation of the final focus magnet. This note describes the recent results obtained on the test benches installed in Annecy [1]. The study covers three main aspects: simulation, measurement and feedback loop. Simulation is important to understand the system to be stabilised, and gives a powerful tool to design a final focusing element with the best characteristics for vibration rejection. To get the know-how required for such a project, the first step is to study a simple case and compare measurements with simulation before moving on to more realistic and complicated systems.

2 Setup description

2.1 Mechanical hardware

We are using a rectangular aluminium beam, 110cm long, 10cm wide and 2cm thick in a free-fixed configuration. The final focus magnet will be close to, or even inside the experiment so that it has to be cantilevered from outside the experiment. Our experimental setup is shown in fig. 1.

Are shown on figure 1 an active TMC table that has been made available by the CERN CLIC team, the aluminium beam clamped on one side, the Endevco sensors, one on the clamping, the other on the beam end, a Güralp geophone and a DAQ running product sofware from Brüel&Kjaer. The TMC table is composed of honeycomb material passively damping the frequencies under 230Hz. The active Stacis2000 feet have geophones measuring the table displacements, and piezoelectric actuators compensating the movements driven by a controller.

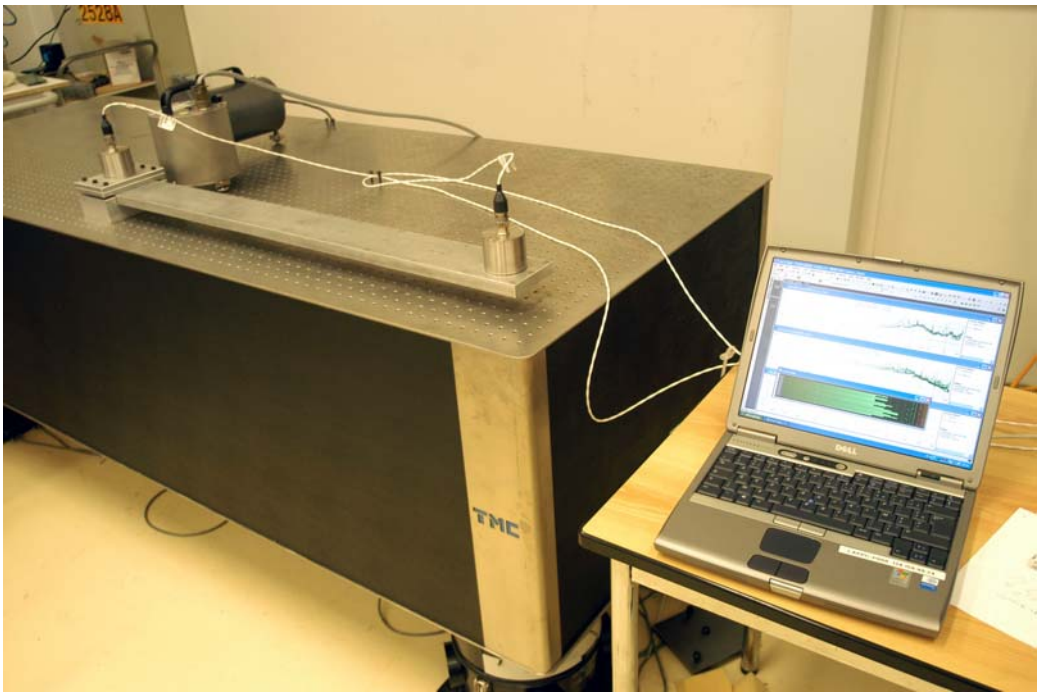

Figure 1: test bench including active table, free-fixed beam, accelerometers, geophones and DAQ running Pulse software.

This table has been used by the CERN-CLIC team to stabilise the top of a CLIC quadrupole model to the nanometre level [2].

2.2 Sensor description

The sensors used for this study are of two types. On the aluminium beam are placed two Endevco Model 86 piezoelectric accelerometers. In addition, a Güralp CMG-40T has been placed on the table as a reference. The characteristics of the sensors are given in table 1.

Sensors	**Calibration for 1V**	**Frequency range**	**Type**
Güralp CMG-40T	±12.5mm/s	0.033-50Hz	Pick-up coil
Endevco 86	0.1g	0.01-100Hz	Piezoelectric

Table 1: Sensor characteristics.

The first step was to characterise the sensors. Ground motion measurements were performed, since it is an important component of the excitation of the aluminium beam on the table. Figure 2 shows the coherence between two identical sensors, placed side by side on the ground, measuring ground motion. The coherence has been determined following equation (1) (more details can be found in ref [3]).

$$C(f) = \frac{\left|\Re e(\langle \tilde{v}_1(f)\tilde{v}_2^*(f)\rangle)\right|}{\sqrt{\left|\langle \tilde{v}_1^*(f)\rangle\langle \tilde{v}_2^*(f)\rangle\right|}} \qquad (1)$$

where v_1 and v_2 are the sensor outputs, $\tilde{v}_1$ and $\tilde{v}_2^*$ the discrete Fourier transforms, * indicating the complex conjugate.

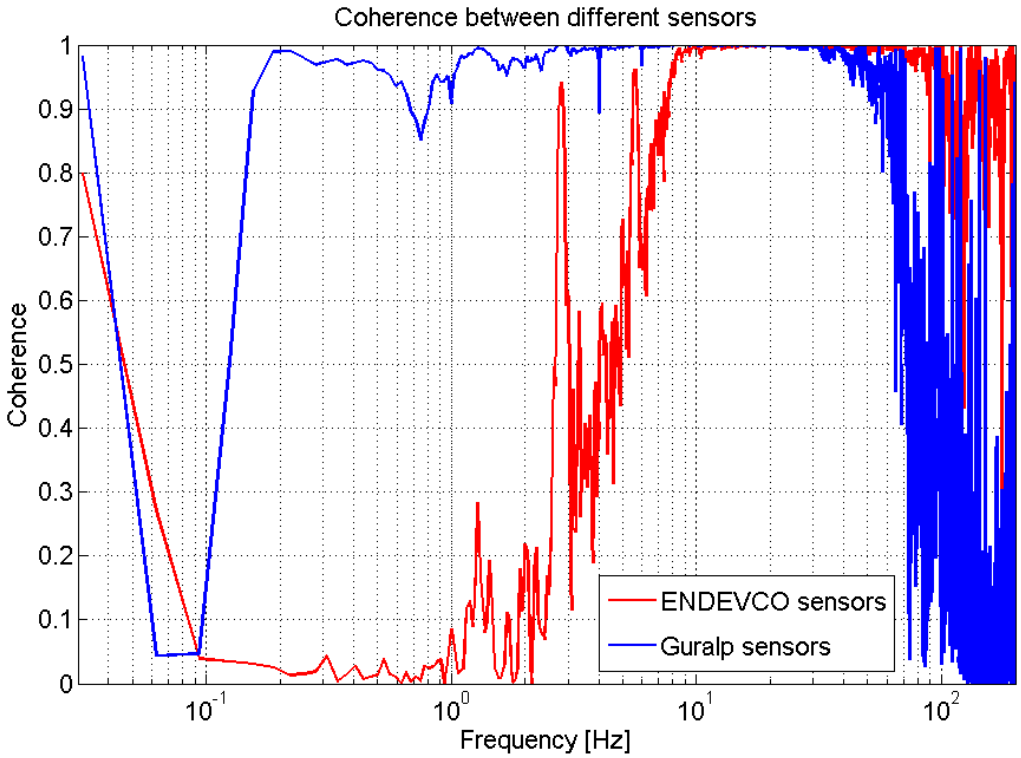

Figure 2: Coherence between two identical sensors. The red curve shows the result for two Endevco accelerometers, and the blue curve for two Güralp sensors.

The ENDEVCO accelerometers show a drop in coherence below 7 Hz. At low frequencies, the ground motion has a very low acceleration amplitude, and is below the accelerometer resolution. On the other hand, the Güralp sensors measure the ground motion velocity. The amplitude of this signal is sufficiently high to be above this sensor's resolution.
The sensor resolutions have been determined following equation (2) and are shown in figure 3.

$$PSD_c(f) = (1 - C(f))\sqrt{PSD_1(f)PSD_2(f)} \quad (2)$$

PSD_c is the Integrated Corrected Difference, the PSD_1 and PSD_2 respectively the Power Spectral Density of the first and second sensor used for the study, and C(*f*) the coherence between the two sensors.

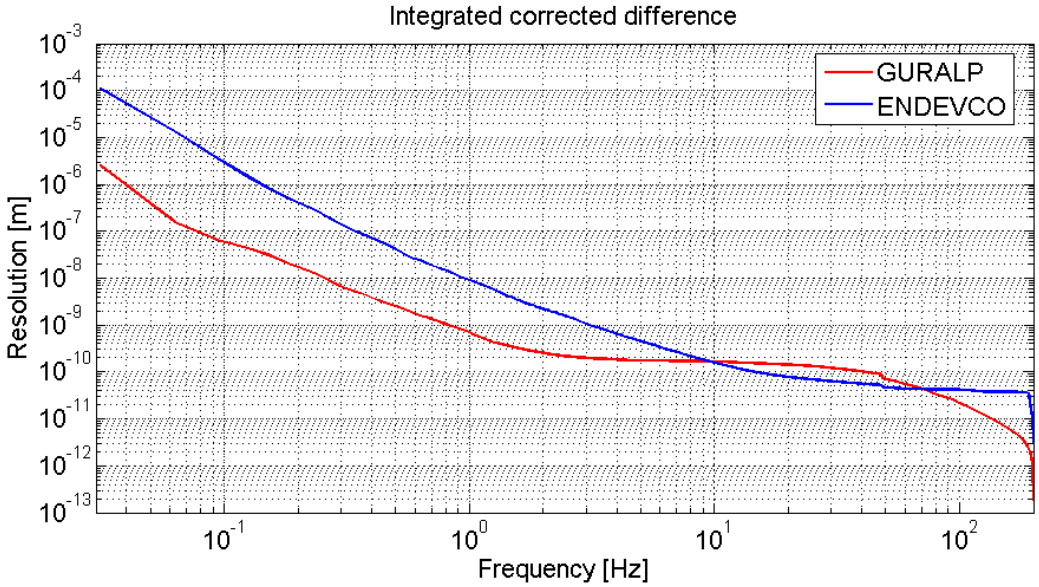

Figure 3: Sensor resolution for the Endevco accelerometers and the Güralp geophones.

Notice that above 1 Hz, the Güralp sensors can measure below the nanometre.
The displacement RMS of the ground measured by the Güralp sensor on top of the table has been measured and determined following equation (3).

$$RMS(f) = \sqrt{\sum_{f}^{f_{max}} PSD(f)df} \quad (3)$$

Figure 4 shows the measurement with the feedback loop of the active table turned on, and the feedback loop turned off. For comparison, at 4 Hz, the displacement on top of the table is 10nm, whereas when the feedback loop is on, this displacement is reduced to 1nm. These measurements reproduce the results shown in [2].

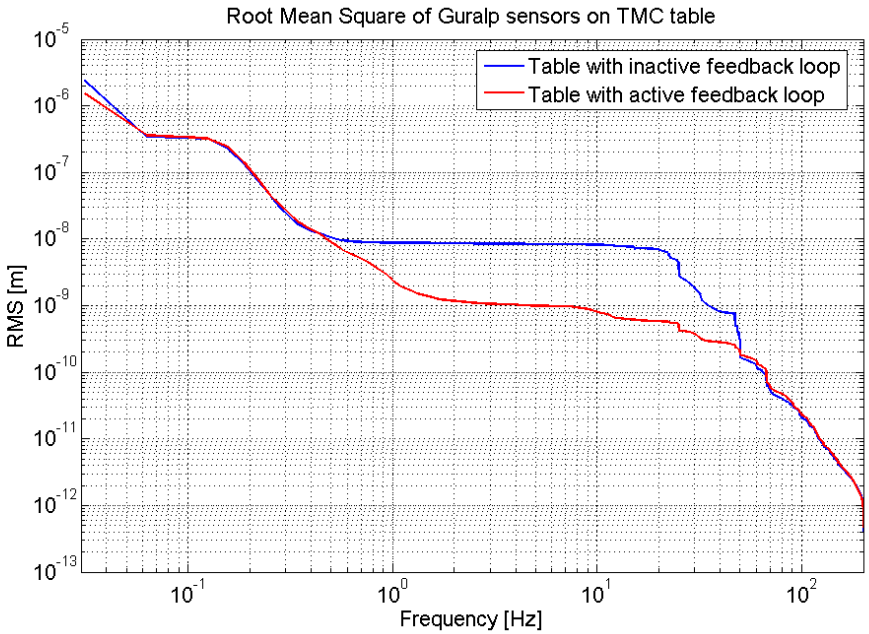

Figure 4: Displacement RMS of the ground measured by the Güralp sensor on top of the table. The two curves show the result for a measurement on the inactive table and on the active table.

3 Finite element simulation

The numerical part of this study is performed with the finite element code SAMCEF. Thanks to this software it is possible to perform not only modal analysis, but also dynamic response predictions.

3.1 Modal analysis

The aim of this simulation is to obtain the different eigenfrequencies and the corresponding mode shapes of a given structure. In our case the structure is a free-fixed beam made of aluminium, whose geometrical characteristics are the following:

length = 1000 mm
width = 100 mm
thickness = 20 mm

The parameters used in the finite element model, are listed below:

E = 74000 MPa	(Young modulus)
ν = 0.3	(Poisson's ratio)
ρ = 2825 kg/m^3	(density)

At last, given that thickness is a small dimension compared with the others, we opted for a meshing composed of shell finite elements. Then SAMCEF can solve the eigenvalue problem and compute the eigenfrequencies and their corresponding vibration modes. Note that the analyzed structure is assumed to be without damping. The computed eigenfrequencies, are listed in table 2. The measurements were done with a smart hammer set-up by Bruel&Kjaer. Figure 5 shows the difference between measurements and calculations.

	1	2	3	4	5	6
Mode description	Z - Flexion	Y - Flexion	Z - Flexion	Z - Flexion	Torsion	Y - Flexion
Experimental frequencies	16 Hz	72 Hz	97 Hz	269 Hz	281 Hz	428 Hz
Numerical frequencies	16 Hz	74 Hz	102 Hz	286 Hz	302 Hz	456 Hz

Table 2: Measured and calculated eigenfrequencies of the free-fixed aluminium beam.

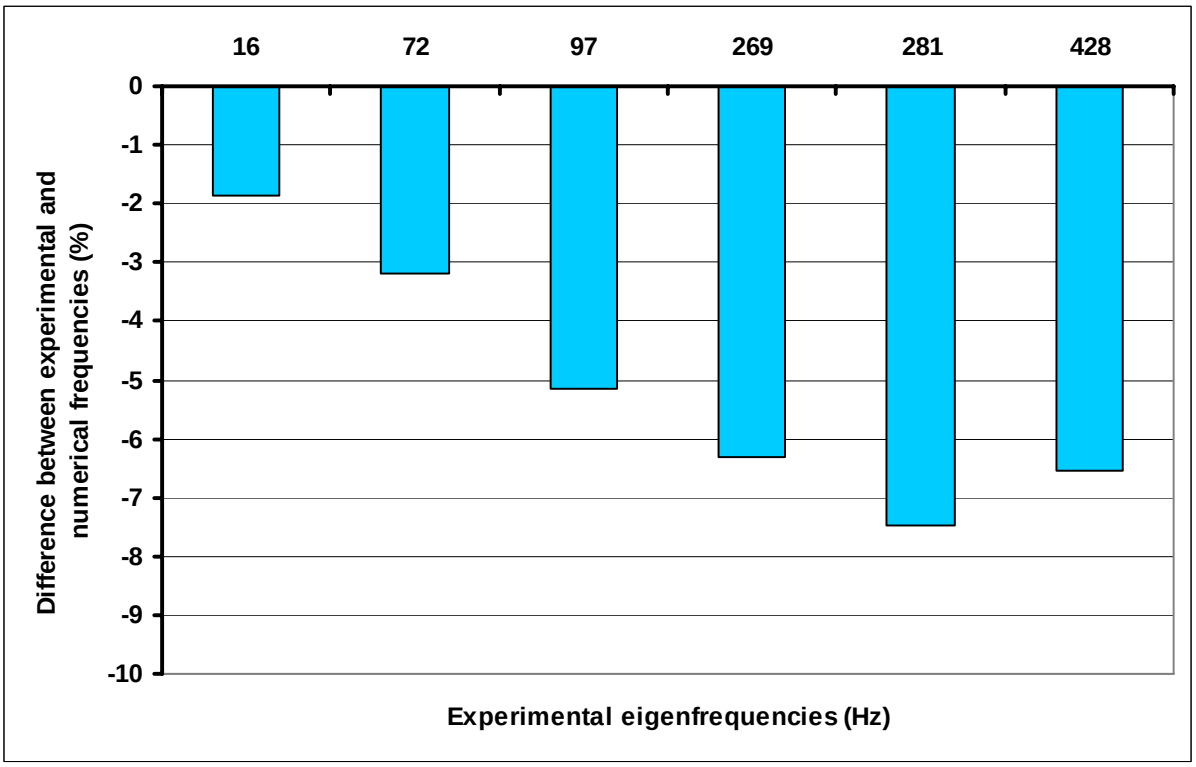

Figure 5: Comparison bar graph of measured and calculated frequencies.

Moreover, the first and the third mode shapes look as follows:

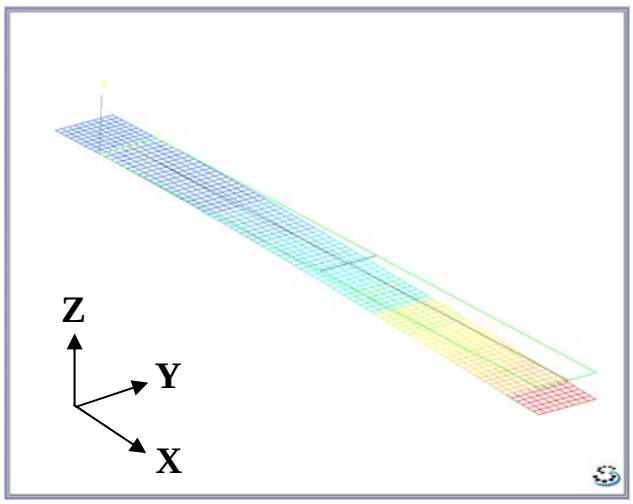

Figure 6: First mode shape

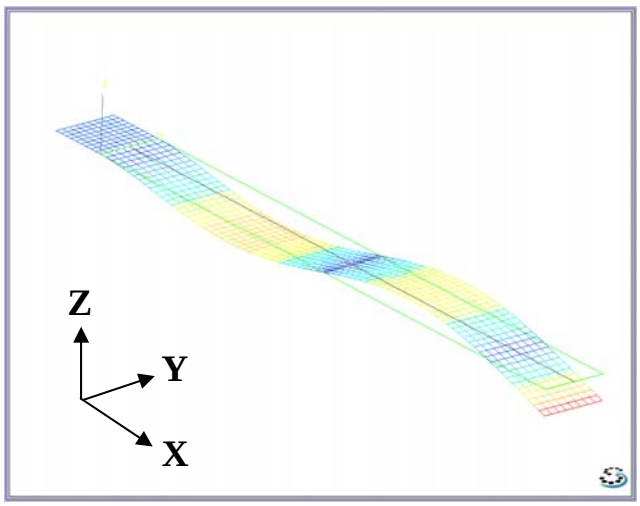

Figure 7: Third mode shape

Note that, in order to obtain better results in terms of frequency, the simulation should include the model of the clamping system, which does not ideally clamp the different degrees of freedom of the structure. As a result, the modelled beam is stiffer than the experimental one. In addition, damping is not taken into account in the model for this calculation. These are the reasons why the computed frequencies are higher than the experimental ones.

3.2 Dynamic response

This kind of simulation is used to get the structural response (in acceleration, velocity or displacement terms) under an external perturbation. In the case of this study, the excitation is the ground acceleration as a function of time. The results are obtained from the computation of the fundamental equations of motion. In order to solve the system made of differential equations, SAMCEF uses the implicit iterative scheme of Newmark. Finally the results are, for instance, accelerations or displacements along the structure, as a function of time.
The model used to perform this simulation is the same as for modal analysis, except that it is now possible to introduce structural damping. An ad doc value of 0.1% of damping was introduced for the first two modes.
The aim of this simulation is to compare the numerical prediction of the motion of the free beam extremity with the experimental one. The latter is measured with the Endevco accelerometer. Therefore, a lumped mass of 830g, located at the beam's edge, is introduced in the model to simulate the accelerometer when computing the dynamic response.
The results of the simulation are given in figure 8.

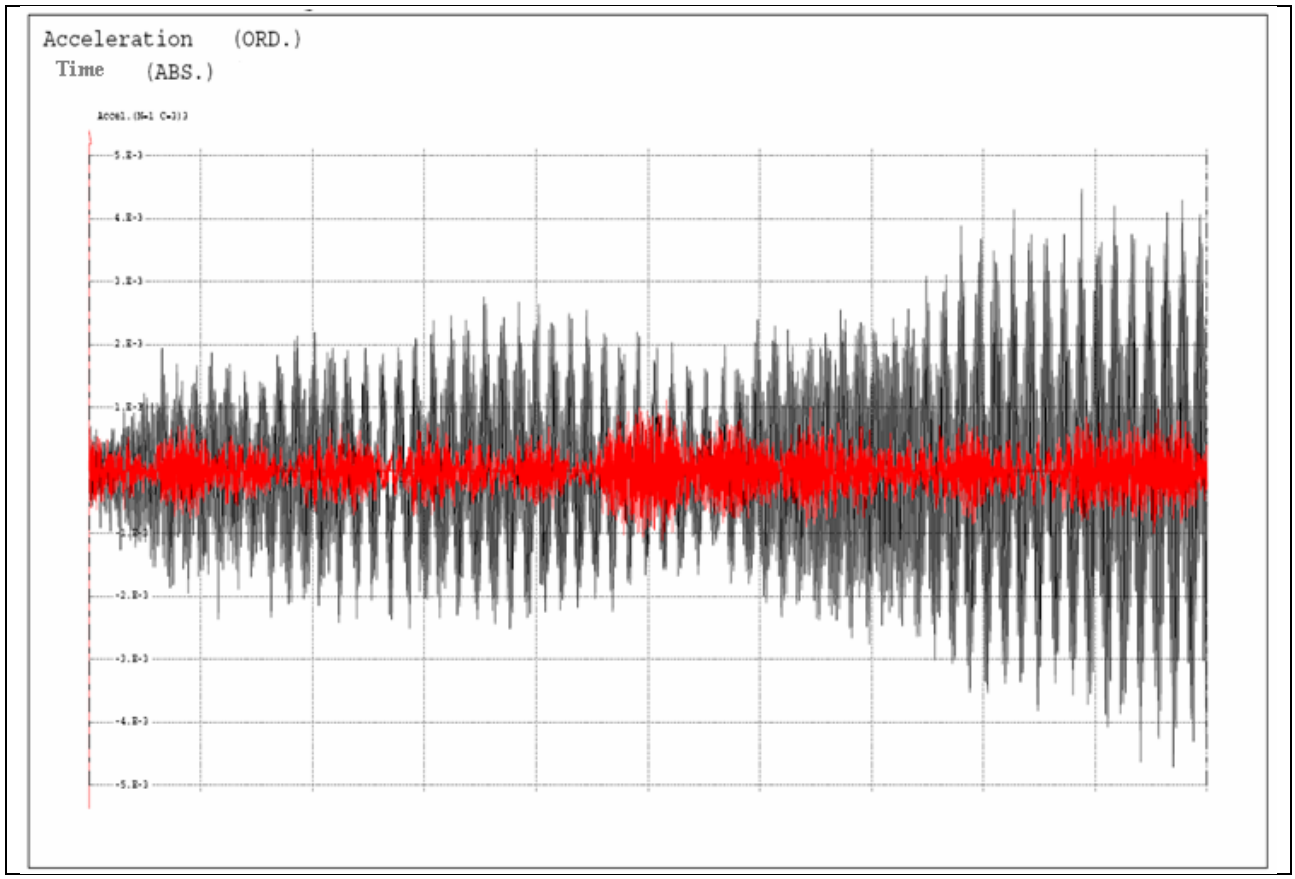

Figure 8: Acceleration calculated on the free-end of the beam (black curve) when excited by the acceleration on the clamping measured by an accelerometer (red curve).

Acceleration of the clamping system as measured, (red curve), and acceleration of the free extremity of the beam (black curve) as computed, are superimposed in order to compare their amplitudes. The duration of the analysis is 8 seconds (X-axis), whereas the acceleration scale is 10^{-3} m.s^{-2} (Y-axis). Note that measured and calculated accelerations correspond to the vertical Z-axis component. Thus only Z-flexion modes are excited. Moreover, acceleration is amplified along the fixed-free beam. The same conclusion could be made for velocity and displacement along the structure.
Finally, the next step consists in the comparison between the numerical predictions (previous results) with the experimental dynamic response.

4 Comparison between vibration measurements and simulation

The measurements are compared to finite element analysis. This will enable us to build mechanical models of our accelerator components and ultimately help in the design of the accelerator parts by optimizing the component, but also by optimizing the actuator, support and sensor position.

4.1 Dynamic response of the free-fixed beam

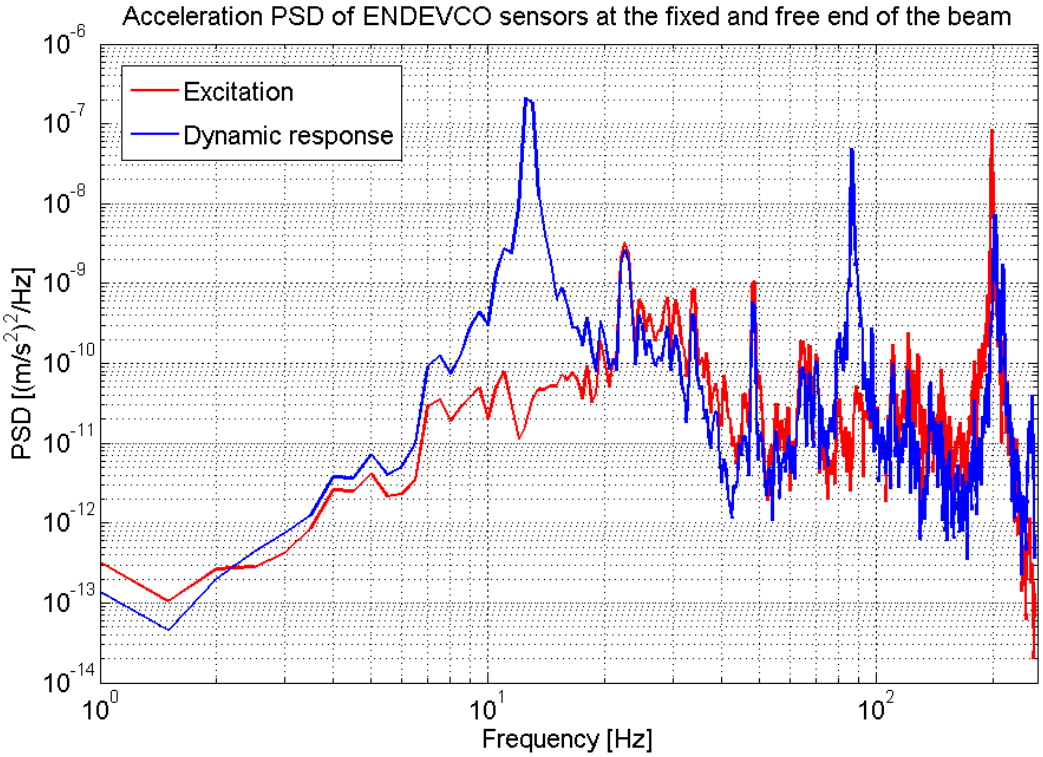

Figure 9: Red curve gives the excitation on the clamping and the blue curve shows the dynamic response.

The accelerometer placed on the free extremity of the beam, measures the dynamic response (cf. test bench shown on Figure 1).
Peaks at 13Hz and 90Hz, shown on figure 9, correspond to the first two Z-flexion modes. That is why acceleration is greatly amplified along the structure. Figure 10 shows the measurement obtained at the free end of the beam and the result of the simulation using as

input the excitation as shown in figure 9. Stiffness has been adjusted, and some damping of 0.1% has been included. The agreement is impressive.

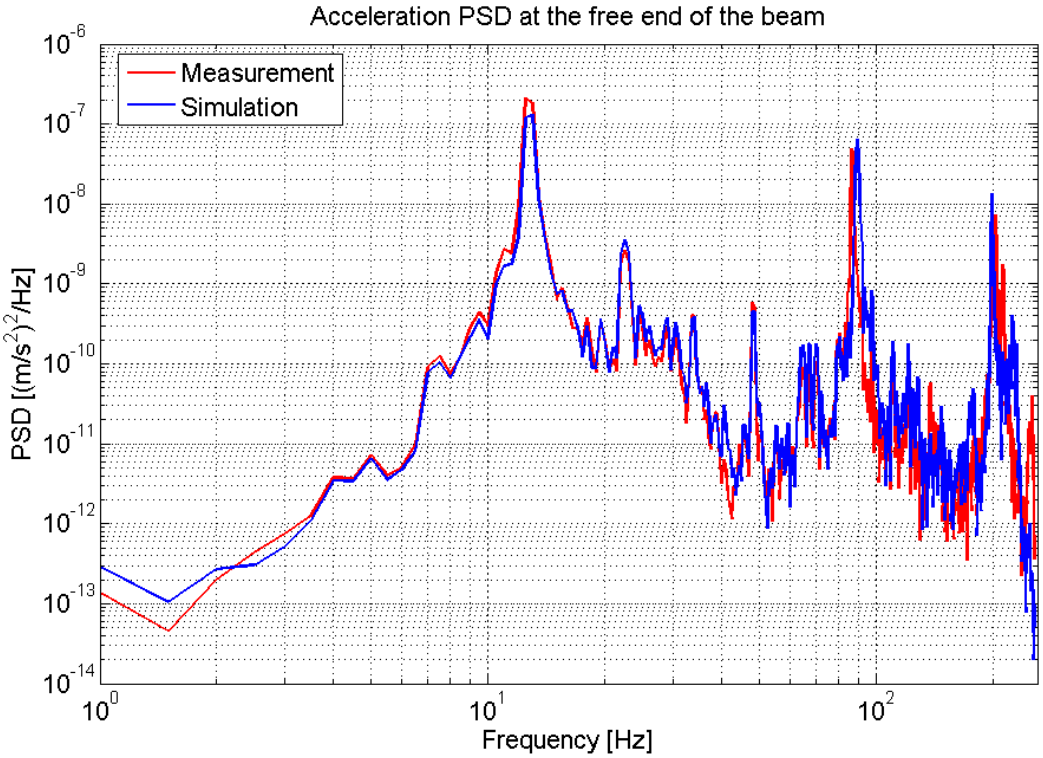

Figure 10: Measurement and simulation result on the free end of the beam using the input shown in figure 9.

4.2 Influence of boundary conditions

Another possibility to damp vibrations of a structure is to add boundary conditions. Typically in the case of a fixed-free beam, it consists in blocking degrees of freedom, for instance in the middle of the beam.
The hereafter results show how to damp Z-flexion modes. The main hypothesis is that the amplitude of the excitation decreases as its frequency increases.
Then, the principle is to block Z-displacements of a beam section, by adding a new support, in order to have a "fixed-simple supported-free" beam. Therefore the Z-flexion eigenfrequencies are shifted to higher values than for a fixed-free beam (cf table 3 and Figure 11)

Localization of the simple support along the 1m beam	no additional support	10cm	20cm	30cm	50cm	65cm
First Z-flexion eigenfrequencies	13 Hz	15 Hz	18 Hz	22 Hz	34 Hz	54 Hz

Table 3: First Z-flexion eigenfrequencies

Note that the probable configuration for the final focus magnet is the fixed free boundary conditions, concerning its extremities. The free part would be inside the detector. That is the reason why simple support above 65cm is not shown here.

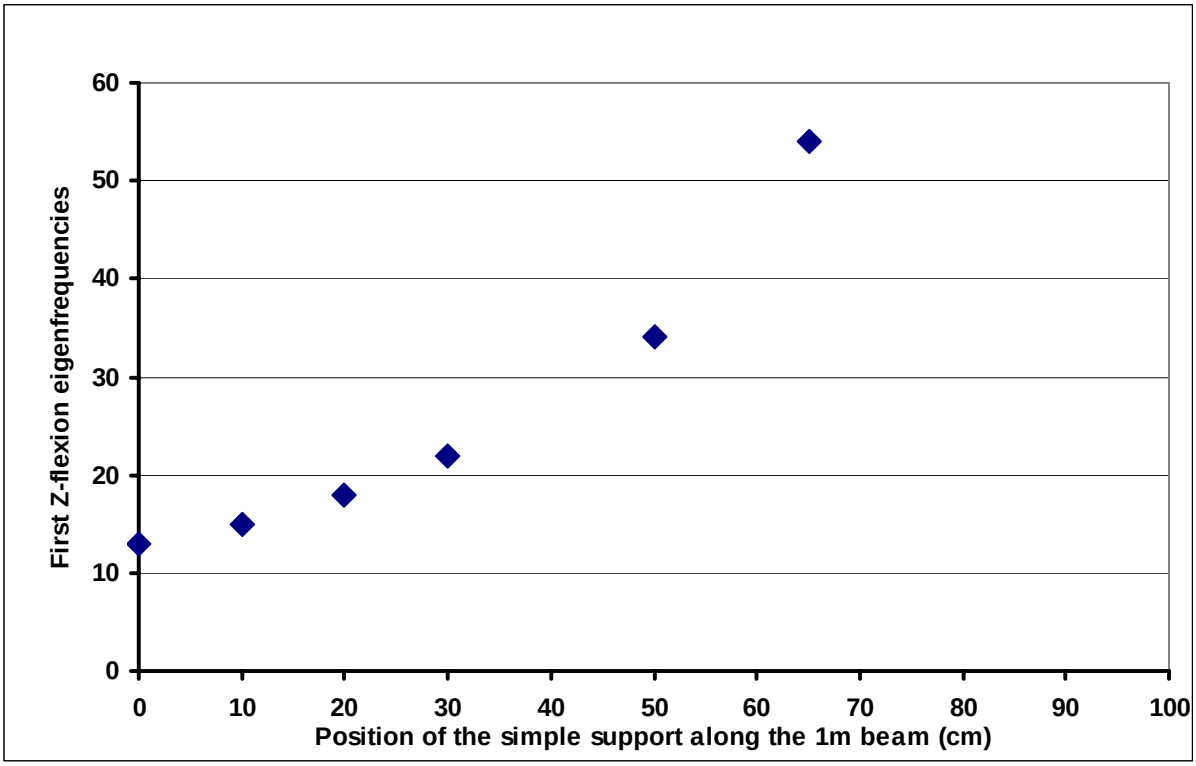

Figure 11: First eigenfrequencies for different distances between the clamping and the extra support.

Comparisons between simulations and measurements have been done for two distances of the support: 20cm and 50cm (cf. figure 12). Results of the simulation are in good agreement with measurements.
It is also very interesting to display the results of the dynamic response of the new beam for the different positions of the support. Figures 13 and 14 show the displacement PSD for measurement and simulation respectively. For both cases, figures show an increase of amplitude for the first resonance peak of each configuration, especially when the support is located at 30cm, and not a reduction as expected. The explanation is the following. The excitation spectrum does not decrease uniformly when the frequency increases (cf. red curve on figure 15). Therefore the excitation peak at 22.5 Hz in the above spectrum excites any structure whose eigenfrequency is around 22.5 Hz. That is exactly the case of the beam with the support at 30cm, but not for the 20cm configuration, since its first eigenfrequency is equal to 18 Hz (cf. table 3). Consequently at 22.5 Hz, the response of the beam is more amplified when the support is fixed at 30cm than at 20cm.
The opposite comment could be made for the peaks at 18 Hz.
Note that these results are explained thanks to the simulation. For this given excitation spectrum (which does not decrease uniformly with frequency), the conclusion could be that, according to figure 13, a beam with no additional support is a better option than with additional support at 30cm, but would not be as efficient as a beam with additional support at 50cm.
In a general way, the best option is to prevent modes to be excited, by shifting them. Obviously, the excitation spectrum must be well known…

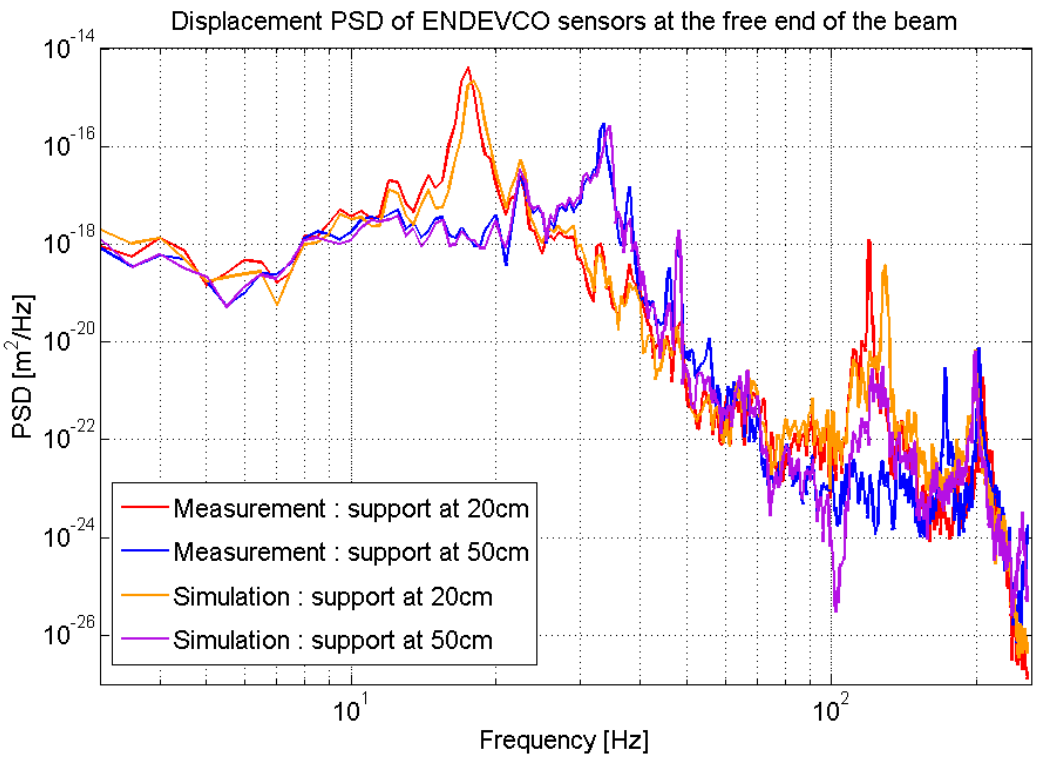

Figure 12: Displacement PSD of the free end.

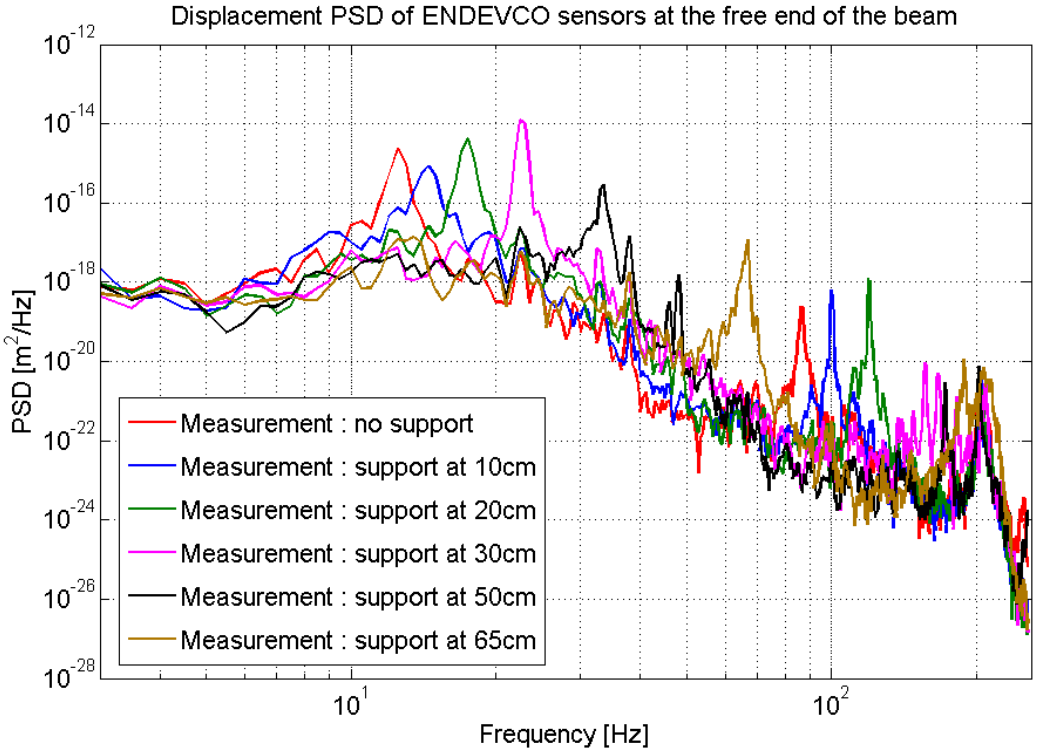

Figure 13: Displacement PSD (measurement).

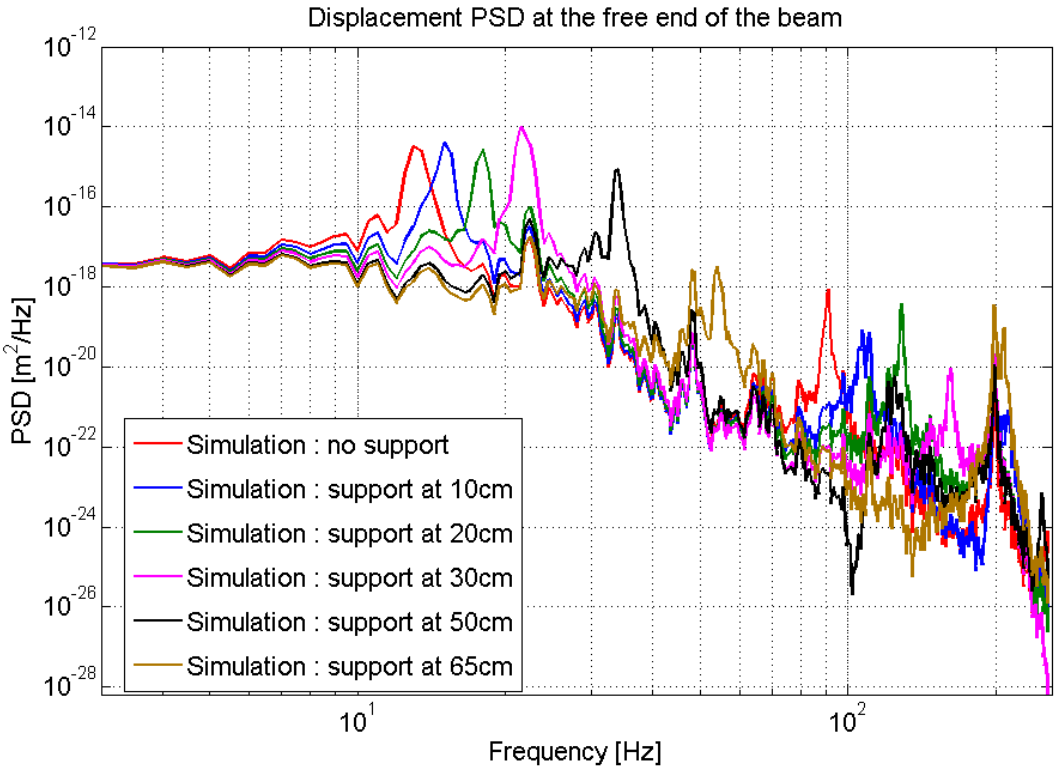

Figure 14: Displacement PSD (simulation).

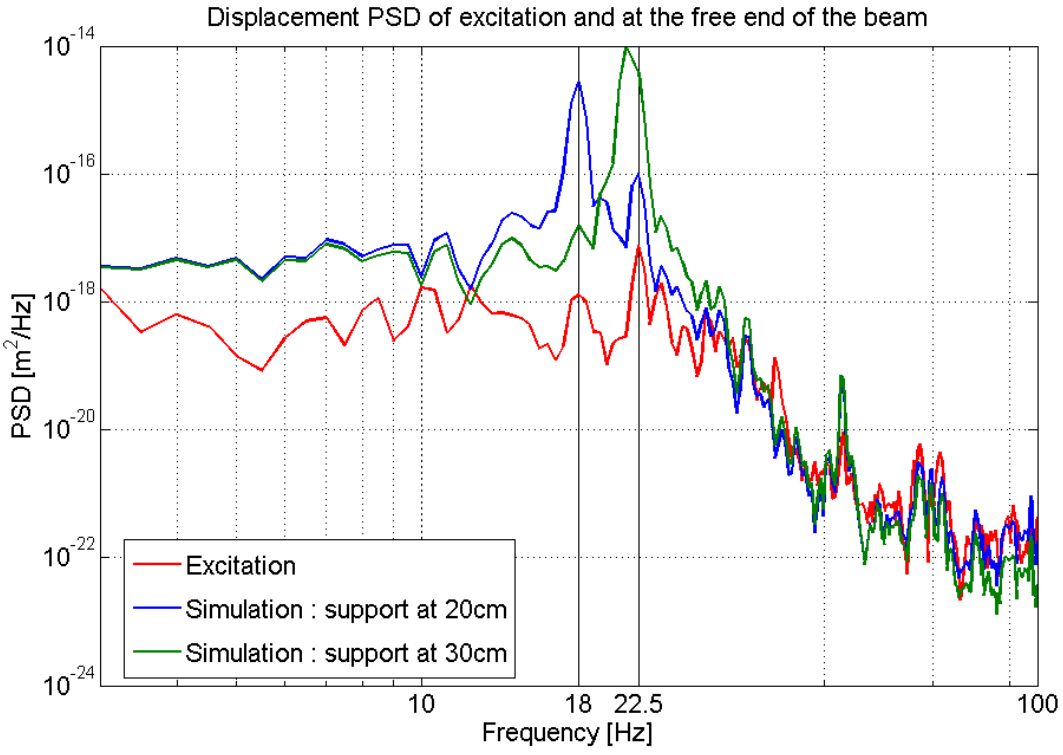

Figure 15: Displacement PSD (excitation and response).

5 Vibration rejection

5.1 Context

The aim of this study is to evaluate the performances of a new algorithm for disturbance rejection. In order to facilitate the analysis, a reduced-size mock-up is used. It should be noticed that due to limitations of PZT actuator capability and of PZT sensor sensitivity, performances are not as good as expected for the future linear collider. However it is possible to analyze the robustness of the algorithm with respect to model mismatch, to evaluate the computational burden and to get an idea of appropriate sampling rate since the frequency ranges are almost equivalent [4],[5].

5.2 Principle

The following reasonable assumptions are made to simplify the design of the control loop:

- main effort is devoted to peaks that appear in the spectral decomposition of the measured signal. These peaks either correspond to resonant modes of the mechanical structure or to particularly amplified modes of the disturbances
- for these peaks, the amplitudes of external disturbances are constant or at least slowly varying with respect to the dynamics of the system/controller
- the peak amplitudes are independent with respect to each other
- the dynamical behaviour of the system is not well known for these particular frequencies

The goal is to create an excitation signal with appropriate amplitude and phase such that the combination of excitation and disturbances is null at the sensor location.
In order to simplify the control scheme synthesis, instead of dealing with amplitude and phase, a decomposition on the (sine, cosine) basis is used. The main advantage is that the rejection problem becomes a linear one [6].
Since resonant peaks are independent, it is possible to treat them separately, and then to add all the contributions in order to get the excitation signal.

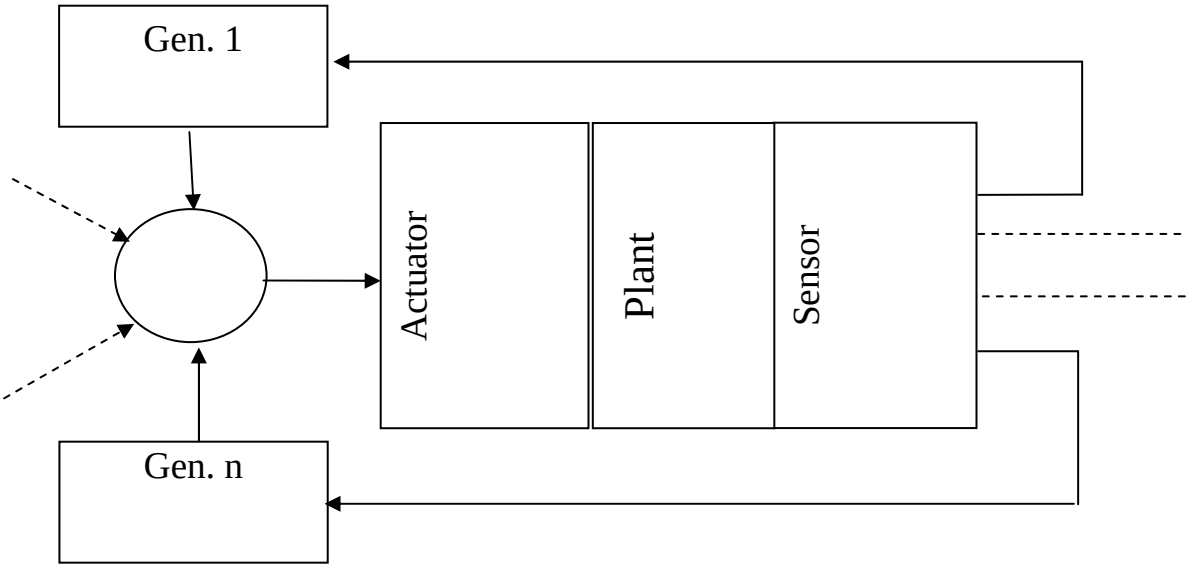

Figure 16. Principle of vibration rejection.

First all interesting frequencies are obtained by means of a Fourier analysis of the measured signal. Since it was shown by simulation tests that the algorithm is very sensitive to frequency

deviation, an on-line procedure will be introduced to adjust these frequency parameters. Two methods are investigated: one of them is based on recursive least mean squares while the other deals with the PLL principle [7].
For each frequency under consideration, the problem consists in controlling a two-input two-output coupled system.
Since for each frequency, the disturbance is supposed to have constant characteristics, the control scheme is based on Proportional-Integral (PI) control loop. This means that control inputs, namely sine and cosine amplitudes of excitation signal, converge to constant value corresponding to the null values of sine and cosine amplitudes of output signal.
Because of coupling effects between both inputs and outputs, a simple PI scheme is not suitable. Introducing state spaces approach, it is possible to get the expected results through static state feedback.
The main functions of the control scheme, whose roles are explained later on, are shown in the following figure.

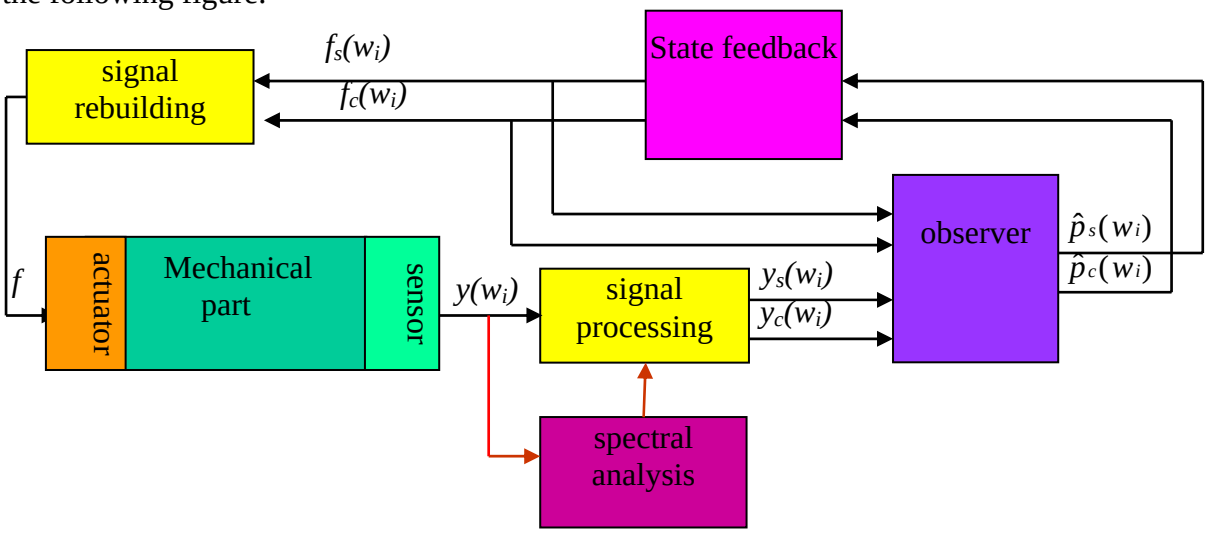

Figure 17. Organization of the algorithm.

A narrow band digital filter whose frequency bandwidth is centred at the considered frequency is used to clean the signal in the vicinity of the frequency.
Then the sine and cosine components are computed by minimizing a least squares criterion. Since this optimization problem is linear with respect to parameters, computations are fast.
The main block of the algorithm is an observer whose role is to estimate the amplitudes (as sine and cosine components) of a virtual disturbance acting on an arbitrary but well defined location in the plant, and creating the same effect on the output as the actual but unknown disturbance.
By means of a predetermined state feedback matrix gain, it is possible to compute the sine and cosine components of the control signal, on the basis of estimated virtual disturbance and matrix gain derived from transfers between virtual disturbance and output on the one hand and control input and output on the other hand.
Knowing sine and cosine components of the control signal for the frequency under consideration, it is easy to build the real-time corresponding contribution.
All these blocks are duplicated as many times as there are peaks to attenuate. Each block parameters are tuned according to the corresponding frequency. All the contributions are summed up in order to create the control signal which feeds the actuator.

5.3 Experimental setup

To test this rejection algorithm, a reduced-size mock-up is used (Fig. 18).

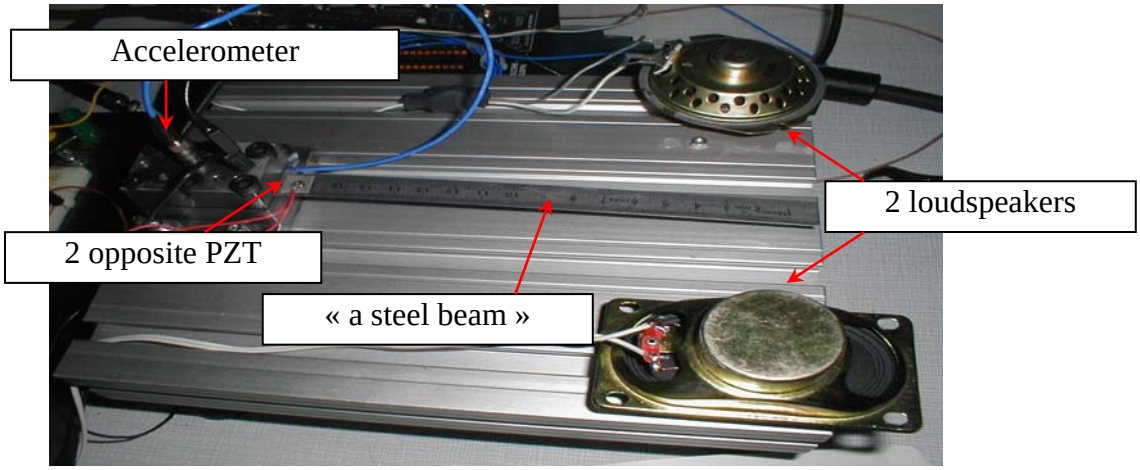

Figure 18. Mock up.

It is composed of:

- a steel beam
- two small loudspeakers as disturbance generators
- one PZT ceramic glued on one side of the beam is used as an actuator, (Fig. 19)
- another collocated PZT ceramic glued on the opposite side is used as a sensor.

Besides, a PC with Matlab software is used to prepare the control algorithm, by means of Simulink and XPC target toolboxes. The final program is downloaded to another PC which is connected to the plant via a National Instruments data acquisition board.
The small size of this experimental set-up induces higher frequency range, and consequently higher sampling rate. This is why, XPC target is used instead of Real Time Windows Target. However the feasibility of the procedure with this mock-up guarantees efficiency when dealing with larger sizes of plants. The actual dimensions were chosen because of easy use of PZT ceramics in the corresponding frequency range.

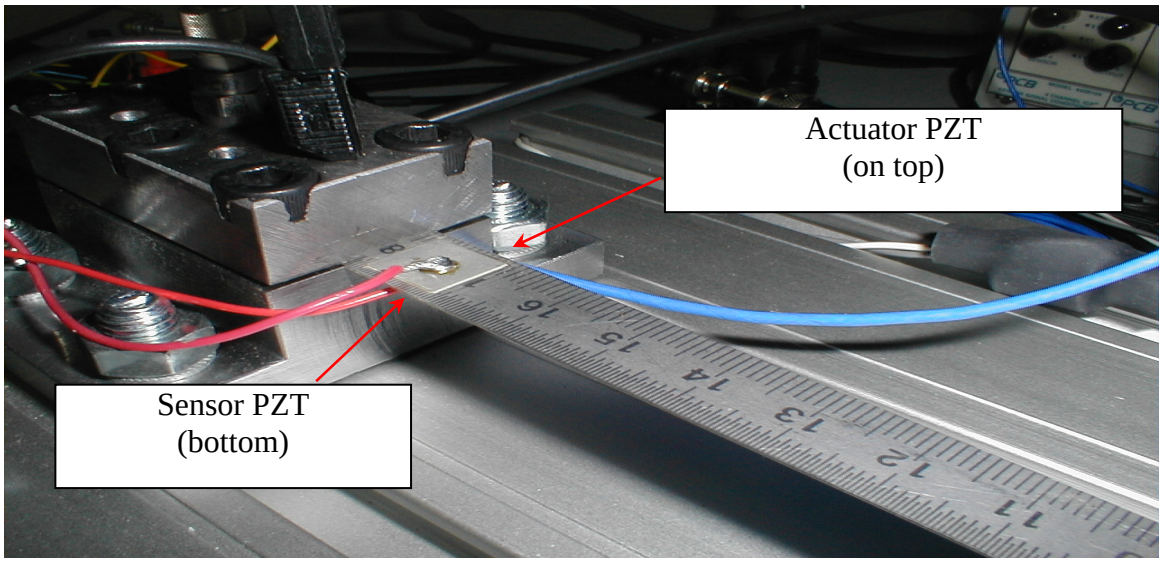

Figure 19. PZT used as actuator. Another PZT on the opposite side is used as sensor.

5.4 Results

Each loudspeaker is fed with a sinusoidal input. A rough harmonic analysis of the system output reveals six resonant modes in the frequency range under consideration: 13, 26, 28, 39, 67 and 82.5 Hz. The corresponding amplitudes are shown in figure 20. One could expect that some of the amplified frequencies come from harmonic components of the excitation inputs created by loudspeakers.

Then six parallel algorithms are activated to elaborate the six contributions of the control signal. When feeding the system PZT actuator with this disturbance, the new spectral decomposition shown in figure 21 is obtained. Note the difference of scale compared to figure 20. To get this result, the required excitation of the PZT actuator has to be as in figure 22. Though not perfect, the result is fairly good:

- peaks are reduced
- no other peak is created

Since the amplitudes are not null, it is necessary to investigate and find some explanations. One of these could be a mismatch between frequencies used in sinusoidal signal generators and actual disturbance frequencies. This is due to quantification of the spectrum, which is related to the sampling rate.

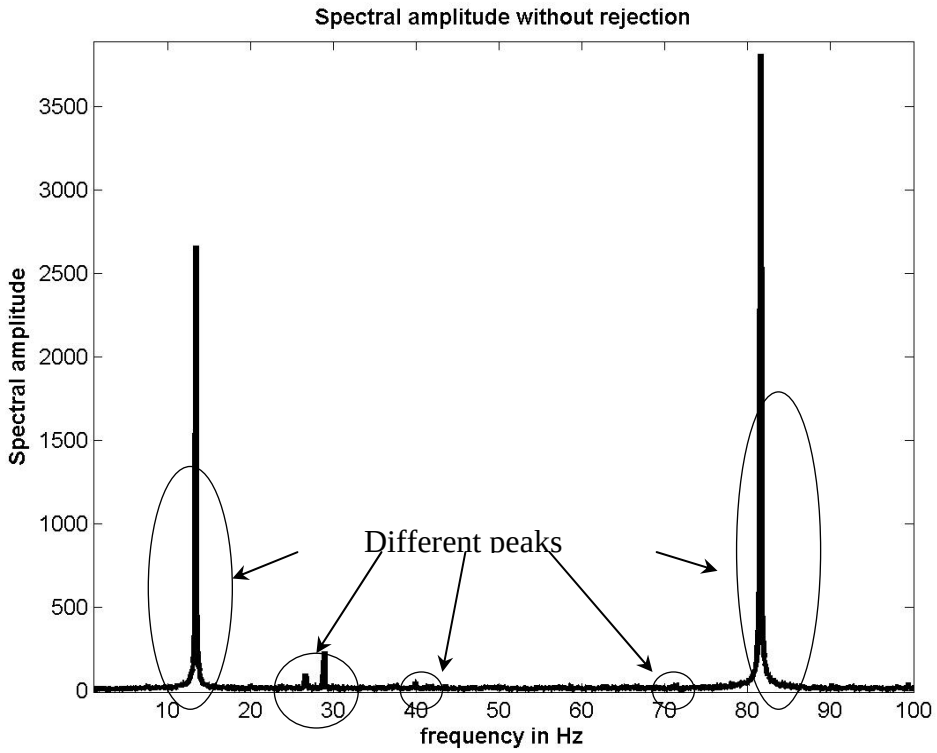

Figure 20. Frequency spectrum before rejection.

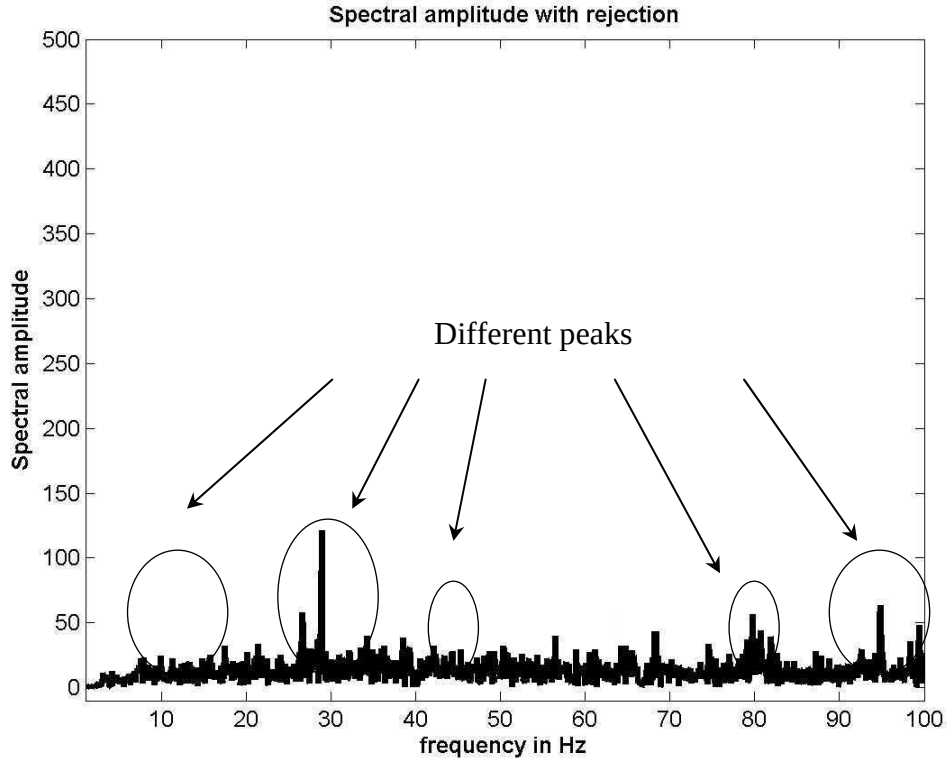

Figure 21. Frequency spectrum after rejection.

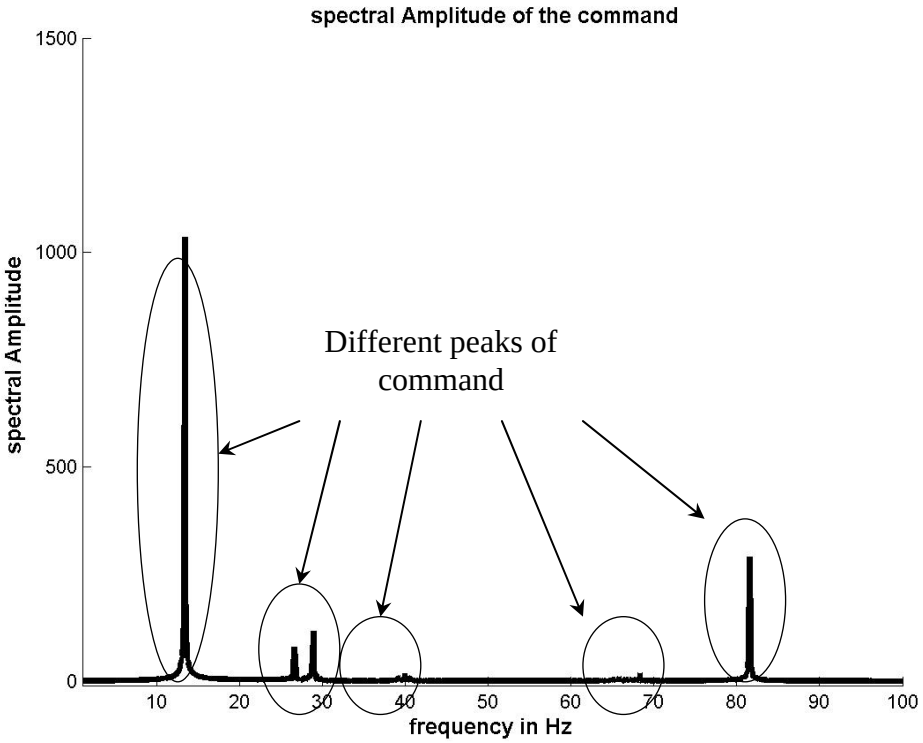

Figure 22. Frequency spectrum of the required PZT command.

6 Conclusion and future prospects

The first step towards a feasibility analysis is to study the three major aspects of active stabilization separately. The velocity sensors that have been characterized on our mock-ups can measure ground motion down to 0.1Hz. The active stabilization table used in this study reduces ground motion from 10nm at 4 Hz to 1nm.
The mechanical modeling gives information about optimal location of sensors and actuators, as well as expected values of eigenmodes that must be considered first by the rejection system and is a powerful tool for further design of test benches and final focus quadrupole.
The six parallel algorithms of the feedback loop reduce considerably the resonance peaks of the reduced-size mock-up while not creating new resonance peaks. More investigation is however needed. This algorithm will be applied to stabilise a larger mock-up, leading to more realistic experimental conditions. In future tests, the active table will globally stabilise in a range of frequencies from 0.5Hz to 50Hz whereas the feedback loop will compensate single strong resonances.
A new mock-up is currently being developed that will have a geometry closer to a final focus quadrupole. Simulation will be used to simulate the whole system: the feedback loop, the sensors, the actuators and their most efficient location. Measurements will be done to validate the whole system in view of active stabilisation for a future linear collider.

Acknowledgement

This work is supported by the Commission of the European Communities under the 6th Framework Programme “Structuring the European Research Area”, contract number RIDS-011899.

References

[1] C. Adloff, B. Bolzon, F. Cadoux, N. Geffroy, S. Géneté, C. Girard, A. Jeremie, Y. Karyotakis, L. Brunetti, J. Lottin, “Vibration stabilization for the final focus magnet of a future linear collider”, Proceedings REM 2005, Annecy-le-Vieux, July 2005.
[2] S. Redaelli, R. Assmann, W. Coosemans, G. Guignard, D. Schulte, I. Wilson and F. Zimmermann, “CLIC magnet stabilization studies,” Proceedings of LINAC2004 TUP88, August 2004, pp. 483–485.
[3] S. Redaelli, “Stabilization of Nanometre-size Particle Beams in the Final Focus System of the Compact Linear Collider (CLIC),” PhD Thesis, Université de Lausanne, 2003, 194 pages, also as CERN-AB-2004-025.
[4] J. Lottin, M. Corduneanu, “Vibration Reduction of magnet quadrupole for beam positioning within a CLIC system”, IMAACA’2004, Gênes, October 2004.
[5] J. Lottin, F. Formosa, V. Cozma, “Experimental evaluation of a new active vibration algorithm”, World IFAC Congress, Praha, July 2005.
[6] M. Bodson and S.C. Douglas, "Adaptive Algorithms for the Rejection of Sinusoidal Disturbances with Unknown Frequency"
[7] B. Wu and M. Bodson, “Multi-channel active noise control for periodic sources-indirect approach".